0026-895X/08/7302-419–430$20.00
MOLECULAR PHARMACOLOGY
Vol. 73, No. 2
39024/3297828
Mol Pharmacol 73:419–430, 2008
Printed in U.S.A.
Copyright © 2008 The American Society for Pharmacology and Experimental Therapeutics

BubR1 Is Required for a Sustained Mitotic Spindle Checkpoint Arrest in Human Cancer Cells Treated with Tubulin-Targeting Pyrrolo-1,5-Benzoxazepines[S]

Lisa M. Greene, Giuseppe Campiani, Mark Lawler, D. Clive Williams, and Daniela M. Zisterer

School of Biochemistry and Immunology, Trinity College, Dublin, United Kingdom (L.M.G., D.C.W., D.M.Z.); Dipartimento Farmaco Chimico Tecnologico, Universita'degli Studi di Siena, Italy (G.C.); and Institute of Molecular Medicine, St. James's Hospital and Trinity College, Dublin, United Kingdom (M.L.)

Received June 20, 2007; accepted November 8, 2007

ABSTRACT

Intrinsic or acquired resistance to chemotherapy is a major clinical problem that has evoked the need to develop innovative approaches to predict and ultimately reverse drug resistance. A prolonged G_2M arrest has been associated with apoptotic resistance to various microtubule-targeting agents (MTAs). In this study, we describe the functional significance of the mitotic spindle checkpoint proteins, BubR1 and Bub3, in maintaining a mitotic arrest after microtubule disruption by nocodazole and a novel series of MTAs, the pyrrolo-1,5-benzoxazepines (PBOXs), in human cancer cells. Cells expressing high levels of BubR1 and Bub3 (K562, MDA-MB-231, and HeLa) display a prolonged G_2M arrest after exposure to MTAs. On the other hand, cells with low endogenous levels of mitotic spindle checkpoint proteins (SK-BR-3 and HL-60) transiently arrest in mitosis and undergo increased apoptosis. The phosphorylation of BubR1 correlated with PBOX-induced G_2M arrest in four cell lines tested, indicating an active mitotic spindle checkpoint. Gene silencing of BubR1 by small interfering RNA interference reduced PBOX-induced G_2M arrest without enhancing apoptotic efficacy. Further analysis demonstrated that PBOX-treated BubR1-depleted cells were both mononucleated and multinucleated with a polyploid DNA content, suggesting a requirement for BubR1 in cytokinesis. Taken together, these results suggest that BubR1 contributes to the mitotic checkpoint induced by the PBOXs.

Microtubules are dynamic polymers that play a fundamental role in a number of cellular functions ranging from cell division to cell motility (Mollinedo and Gajate, 2003). Hence, microtubule-targeting agents (MTAs) represent some of the most clinically successful chemotherapeutic drugs identified to date. Tubulin is the principle component of microtubules. MTAs function by affecting the equilibrium between free tubulin dimers and assembled polymers. Together, MTAs consist of a diverse group of antimitotic drugs that may be subdivided into two distinct categories: those that inhibit microtubule polymerization (e.g., vinca alkaloids and nocodazole) and those that promote microtubule polymerization and subsequent stabilization of the microtubules (e.g., paclitaxel) (Jordan, 2002). The clinical success of the taxanes and vinca alkaloids has evoked a major search for new drugs that perturb mitotic spindle microtubule dynamics and function.

We recently described a novel group of tubulin targeting compounds, namely, the pyrrolo-1,5-benzoxazepines (PBOXs), which are structurally distinct from the aforementioned MTAs (Mulligan et al., 2006). PBOX-6, a representative member of the PBOX compounds, functions by inhibiting microtubule polymerization followed by cell cycle arrest at G_2M and late apoptosis (Mulligan et al., 2006). PBOX-6 induced many of the biochemical hallmarks of apoptosis, including PARP cleavage, cytoplasmic blebbing, DNA fragmentation, and positive tunnel staining (Mc Gee et al., 2002a; Greene et al., 2005). A cell type-specific dependence of caspases on PBOX-6-induced apo-

This study was supported by Science Foundation Ireland.
Article, publication date, and citation information can be found at http://molpharm.aspetjournals.org.
doi:10.1124/mol.107.039024.
[S] The online version of this article (available at http://molpharm.aspetjournals.org) contains supplemental material.

ABBREVIATIONS: MTA, microtubule-targeting agent; PBOX, pyrrolo-1,5-benzoxazepine; PBOX-6, 7-[(dimethylcarbamoyl) oxy]-6-(2-naphthyl)pyrrolo-[2,1-*d*][1,5]benzoxazepine; PBOX-15, 4-acetoxy-5-(-1-(naphthyl)naphtho[2,3-*b*]pyrrolo[2,1-*d*] [1,4]oxazepine; PARP, poly(ADP-ribose) polymerase; APC/C, anaphase-promoting complex/cyclosome; DMEM, Dulbecco's modified Eagle's medium; FCS, fetal calf serum; DMSO, dimethyl sulfoxide; mAb, monoclonal antibody; siRNA, small interfering RNA; PBS, phosphate-buffered saline; PAGE, polyacrylamide gel electrophoresis; TBS-T, Tris-buffered saline, pH 7.6/0.05% Tween 20; PI, propidium iodide; PBST, PBS and 0.1% Triton X-100; ZM447439, N-[4-[[6-methoxy-7-[3-(4-morpholinyl)propoxy]-4-quinazolinyl]amino]phenyl]benzamide.

ptosis was observed (Zisterer et al., 2000; Mc Gee et al., 2002a), a trait shared with paclitaxel (Ofir et al., 2002). As demonstrated with other MTAs, we have shown that activation of c-Jun NH_2-terminal kinase, together with the phosphorylation and inactivation of the antiapoptotic proteins Bcl-2 and Bcl-x_L, are a prerequisite for PBOX-6-induced apoptosis (Mc Gee et al., 2002b, 2004). PBOX-6 induced apoptosis in a wide spectrum of cancer cells without displaying any activity toward normal blood cells (Zisterer et al., 2000; Mc Gee et al., 2001, 2004; Greene et al., 2005). It is noteworthy that, unlike the taxanes, PBOX-6-induced apoptosis is independent of Bcl-2 and Her-2 expression levels (Mc Gee et al., 2004; Greene et al., 2005). Up-regulation of the antiapoptotic Bcl-2 protein and the Her-2 oncogene was previously shown to contribute to paclitaxel resistance (Tang et al., 1994; Yu et al., 1998). Furthermore, PBOX-6 displayed significant antitumor activity in vivo in an aggressive murine model of mammary carcinoma (Greene et al., 2005). The tumor-selective effects of the tubulin-targeting PBOX compounds and apoptotic efficacy in chemotherapeutic resistant cells highlight their potential as anticancer agents.

It is well accepted that tubulin-targeting agents principally function by disrupting microtubule dynamics during mitosis and subsequent activation of the mitotic spindle checkpoint leading to mitotic cell cycle arrest. Exposure to MTAs can induce differential responses in different cell types. Some cells exhibit a sustained mitotic arrest, whereas others only arrest transiently in mitosis and proceed to undergo apoptosis. The mitotic spindle checkpoint monitors both the attachment of chromosomes to the mitotic spindle and the tension across the sister chromatids generated by microtubules. The checkpoint signal is generated at the kinetochore, a large multiprotein subunit that is located on the centromere of each chromosome and mediates the attachment of chromosomes to the mitotic spindle (Cleveland et al., 2003). There is substantial evidence to suggest that the checkpoint prevents cell cycle progression by inhibiting the activity of the anaphase-promoting complex/cyclosome (APC/C) (Acquaviva et al., 2004). The APC/C is an ubiquitin ligase that upon interaction with its coactivator, Cdc-20, targets anaphase inhibitors (securin/Pds1) and mitotic cyclins (cyclin B) for proteasome-mediated degradation (Peters, 2002). This cascade of events ultimately leads to cohesion degradation and chromosomal separation (Peters, 2002; Doncic et al., 2005). Several key mitotic spindle checkpoint proteins (Bub1, BubR1, Mps1, Bub3, Mad1–3) have been identified that bind to Cdc-20 and prevent activation of the APC/C and in doing so inhibit anaphase progression. Logarinho et al. (2004) suggested that spindle checkpoint proteins sense distinct aspects of kinetochore interaction with the spindle, with Mad2 and Bub1 monitoring microtubule occupancy, whereas BubR1 and Bub3 monitor tension across attached kinetochores.

In this study, we sought to determine the effects on BubR1 and Bub3 expression levels after PBOX-induced loss of microtubule tension in a panel of human cancer cells and decipher any correlation with a sustained mitotic arrest. We also characterize the antimitotic properties of PBOX-15, a more potent analog of the recently described tubulin-targeting pyrrolo-1,5-benzoxazepine, PBOX-6.

Materials and Methods

Cells. All cell lines were originally obtained from the European Collection of Cell Cultures (Salisbury, UK). The K562 cells were derived from a patient in the blast crisis stage of chronic myeloid leukemia. HL-60 cells were derived from a patient with acute myeloid leukemia. MDA-MB-231 and SK-BR-3 cells originate from a pleural effusion from patients with metastatic adenocarcinoma of the breast. HeLa cells are cervical adenocarcinoma-derived. K562 cells and HL-60 cells were cultured in RPMI-1640 medium. MDA-MB-231 and HeLa cells were grown in Dulbecco's modified Eagle's medium (DMEM). SK-BR-3 cells were grown in McCoy's 5a medium modified. HL-60 cells were maintained in medium enhanced with 20% FCS, and all other cell lines were grown in media supplemented with 10% FCS. All media were supplemented with 100 units/ml penicillin, 100 μg/ml streptomycin, and 2 mM glutamine. Cells were maintained at 37°C in 5% CO_2 in a humidified incubator.

Reagents. PBOX-6 (7-[(dimethylcarbamoyl) oxy]-6-(2-naphthyl)pyrrolo-[2,1-*d*][1,5]benzoxazepine) and PBOX-15 (4-acetoxy-5-(-1-(naphthyl)naphtho[2,3-*b*]pyrrolo[2,1-*d*] [1,4]oxazepine) were synthesized as described previously (Campiani et al., 1996) and dissolved in ethanol. Structures of the PBOX compounds were described by Mulligan et al. (2006). Nocodazole was purchased from Sigma Chemical Co. (Poole, Dorset, UK) and dissolved in sterile DMSO. All compounds once dissolved in the relevant solvent were stored at −20°C. Cell culture medium was purchased from Invitrogen (Carlsbad, CA). L-Glutamine and penicillin/streptomycin were supplied from Sigma. The anti-Bub3 mouse monoclonal antibody (mAb) and the mouse anti-BubR1 mAb were purchased from BD Transduction Laboratories (Cowley, UK). The anti-actin mAb and anti-tubulin antibodies were obtained from Merck Biosciences (Nottingham, UK). Fluorescein isothiocyanate anti-mouse and Cy3 anti-sheep antibodies were purchased from Jackson Immunoresearch Laboratories (Suffolk, UK). The enhanced chemiluminescence reagent was obtained from GE Healthcare (Chalfont St. Giles, Buckinghamshire, UK). For small interfering RNA (siRNA) experiments, the siRNA duplexes were supplied from Ambion (Huntingdon, UK), and the oligofectamine transfection reagent was purchased from Invitrogen (Paisley, UK). All other chemicals were obtained from Sigma.

Western Blot Analysis. After treatment, whole-cell pellets were washed in PBS, resuspended in 60 μl of PBS, lysed by the addition of 60 μl of 2× Laemmli buffer (1× = 30 mM Tris base, pH 6.8, 2% SDS, and 10% glycerol) and briefly sonicated. Homogenates were quantified by the Markwell protein assay before addition of reducing agent (50 mM dithiothreitol). Samples were boiled for 3 min, and equal amounts of protein were separated by SDS-PAGE and electroblotted to polyvinylidene difluoride membrane. The blots were stained in 0.1% Ponceau S (w/v) in 5% acetic acid (v/v) to ensure equal transfer. Membranes were briefly washed in Tris-buffered saline, pH 7.6, and 0.05% Tween 20 (TBS-T) and blocked at room temperature in TBS-T containing 5% (w/v) dried milk (blocking buffer). After 1 h, the blots were then incubated overnight at 4°C in 1 μg/ml primary antibody diluted in 5% blocking solution. Blots were then washed 3 × 10 min in TBS-T and incubated for 1 h at room temperature in a 1:1000 dilution of horseradish peroxidase-conjugated secondary antibody. Blots were again washed 3 × 10 min in TBS-T and developed by enhanced chemiluminescence.

Drug Treatment. For the suspension cells, logarithmically growing cells were seeded at 200,000/ml (K562) and 300,000/ml (HL-60) in sterile plastic T-flasks. For adherent cells, cells were seeded at a density of $3.4 \times 10^4/cm^2$ (SK-BR-3), $4 \times 10^4/cm^2$ (MDA-MB-231), and $9.2 \times 10^3/cm^2$ (HeLa) for 24 h before drug treatment. Cells were left untreated or treated with solvent control or with the designated concentration of drug for the specified period. At the end of the incubation period, cells were harvested by centrifugation at 600*g* for 10 min at room temperature and prepared for subsequent analysis as detailed below.

Determination of DNA Content. The flow cytometric evaluation of cellular DNA content was performed as described previously (Greene et al., 2005). In brief, after treatment of adherent cell lines, floating cells were collected and then pooled with attached cells removed by trypsinization. Once collected, all cell types were then

centrifuged at 800*g* for 10 min and resuspended in ice-cold PBS (200 μl). Cells were then fixed by a drop-wise addition of 70% ethanol/PBS (2 ml) while gently vortexing the cells. After fixation for at least 1 h at −20°C and addition of 0.25% FCS, cells were again centrifuged and resuspended in PBS containing 10 μg/ml RNase A and 100 μg/ml propidium iodide (PI). Cells were then incubated for 30 min in the dark at 37°C. The PI fluorescence was measured on a linear scale using a FACSCalibur flow cytometer (Becton Dickinson, San Jose, CA). The amount of PI fluorescence is directly proportional to the amount of DNA present in each cell. The relative content of DNA indicates the distribution of a population of cells throughout the cell cycle. For example, cells in G_0G_1 are diploid and have a DNA content of 2N. Cells with the G_2M phases have a DNA content of 4N, whereas cells in S phase have a DNA content between 2N and 4N. Apoptotic cells are subdiploid (<2N), and polyploid cells have a >4N DNA content. Data collection was gated to exclude cell debris and cell aggregates. At least 10,000 cells were analyzed per sample. All data were recorded and analyzed using the CellQuest software (Becton Dickinson).

siRNA Transfection. In this study, we used a validated siRNA duplex to target the BubR1 sequence 5′-GGUGGGAAGGAGAGUAAUATT-3′ (Ambion). A scrambled RNA duplex was used as a control (5′-AGGGUAGUAGGAGAGAUGATT-3′). The selected siRNAs were BLAST searched against the human genome sequence to ensure only one gene was targeted, whereas the control scrambled siRNA sequence used has no known overlap. Cells were seeded at density of $7.2 \times 10^3/cm^2$ (HeLa) and $1.8 \times 10^4/cm^2$ (MDA-MB-231) in DMEM without antibiotics. After 24 h, the transfection was carried out on 50% confluent cells in Optimen medium using oligofectamine transfection reagent (Invitrogen) in accordance with the manufacturer's instructions. The siRNA complexes were removed after 4 or 24 h and replaced with DMEM supplemented with 20% FCS. Cells were analyzed 24 to 120 h after transfection.

Immunofluorescence and Confocal Microscopy. For immunofluorescence, HeLa cells were grown on poly-L-lysine-coated coverslips. After treatment, cells were washed twice with PBS, washed once with microtubule-stabilizing buffer (100 mM PIPES, pH 6.8, 1 mM MgCl, 0.1 mM $CaCl_2$, 0.1% Triton X-100) at room temperature, then fixed for 10 min in 4% formaldehyde diluted in the microtubule-stabilizing buffer. After washes in PBS and 0.1% Triton X-100 (PBST), cells were blocked in 5% nonfat dried milk (Marvel; Premier Foods, St. Albans, UK) diluted in PBST (blocking buffer). Cells were then incubated with primary antibodies, mouse anti-tubulin (DM1A; 1:20) and sheep anti-BubR1 (SBR1.1; 1:1000) (kindly provided by Dr. Stephen Taylor, School of Biological Sciences, University of Manchester), for 1 h at room temperature. After washes in PBST, cells were incubated with secondary antibodies (fluorescein isothiocyanate anti-mouse and Cy3 anti-sheep) for 1 h at room temperature. After washes in PBST, the cells were stained with Hoechst 33258 at 1 μg/ml in PBS for 5 min, mounted in 4% propyllgallate in PBS/glycerol. Projected images from a *z*-series of 15 to 22 stacks of confocal images acquired at 0.6 μM intervals were captured using the Olympus 1×81 microscope (Olympus, Tokyo, Japan) coupled with Olympus Fluoview version 1.5 software. All images in each experiment were collected on the same day using identical parameters.

Statistical Analysis. The statistical analysis of experimental data were performed using a Student's paired *t* test, and results are presented as mean ± S.E.M. A value of $P < 0.05$ was considered to be significant.

Results

Effects of PBOX-15, a Novel Pyrrolo-1,5-Benzoxazepine, on the Cell Cycle and Apoptosis in K562 Cells. We have previously reported that PBOX-6, a representative member of the proapoptotic subset of PBOX compounds, induced apoptosis in K562 cells after a prolonged G_2M cell cycle arrest (Mulligan et al., 2006). In this manuscript, we describe a novel more potent antimitotic member of the PBOX series, PBOX-15. PBOX-15 (IC_{50}, 0.2 μM) was 11-fold more effective at inducing a G_2M cell arrest in K562 cells than PBOX-6 (IC_{50}, 2.2 μM) (Fig. 1A). As observed in the present study and previously with PBOX-6 (Mulligan et al., 2006), PBOX-15-induced G_2M cell cycle arrest is detected as early as 2 h, peaks at 16 h, is sustained up to 24 h, and finally begins to decline at 48 h (Fig. 1B). Again, as previously shown with PBOX-6, the prolonged G_2M cell cycle arrest induced by PBOX-15 was followed by late apoptosis at 48 h (Fig. 1C).

Phosphorylation of the Mitotic Spindle Checkpoint Protein BubR1 Was Associated with a Sustained G_2M Cell Cycle Arrest after Treatment with Tubulin-Targeting PBOX Compounds in K562 Cells. As already discussed, PBOX-induced apoptosis in K562 cells is a delayed

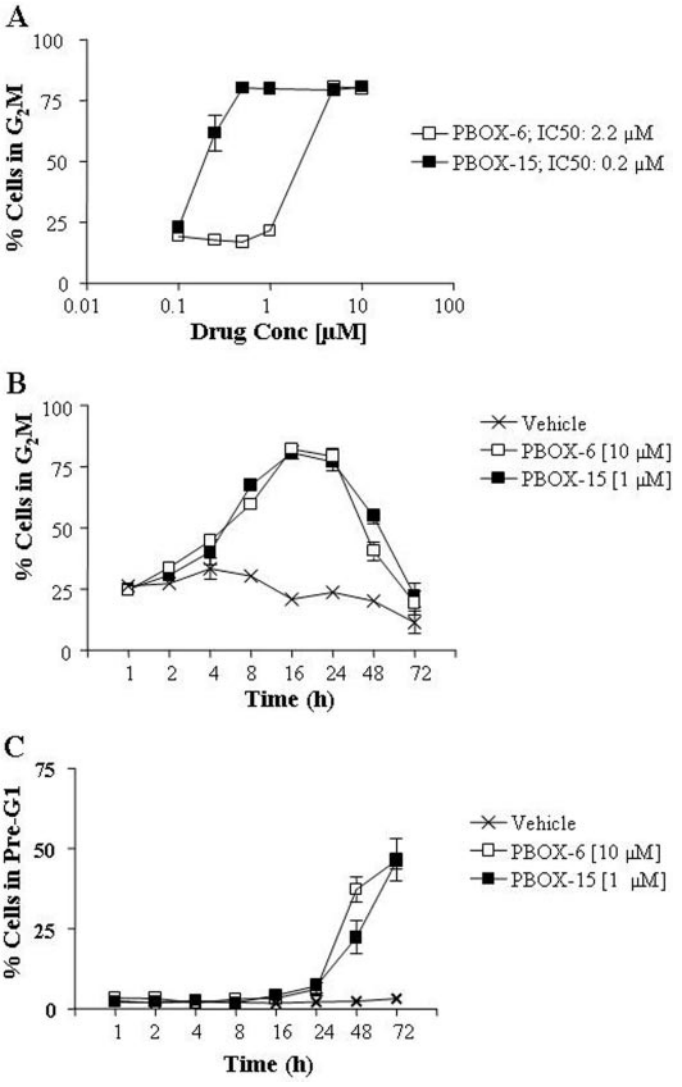

Fig. 1. PBOX-15 is a more potent antimitotic analog of PBOX-6. Logarithmically growing K562 cells were exposed to vehicle [0.2% ethanol (v/v)], PBOX-6 or -15 (0.1–10 μM) for 16 h (A), or PBOX-6 (10 μM) or PBOX-15 (1 μM) for 1 to 72 h (B and C). Cells were then fixed, stained with PI, and analyzed by flow cytometry. Cell cycle analysis was performed on histograms of gated counts per DNA area (FL2-A). The number of cells with <2N (pre-G_1), 2N (G_0G_1), 4N (G_2M), and >4N (polyploid cells) DNA content was determined using the Cell Quest software. The pre-G_1 peak is indicative of apoptosis. Values represent the mean ± S.E.M. for at least three separate experiments. The absence of error bars indicates that the error was smaller than the size of the symbol.

event after a prolonged G_2M cell cycle arrest. In this study, Western blot analysis was used to determine whether the mitotic spindle checkpoint proteins BubR1 and Bub3 are associated with PBOX-induced G_2M cell cycle arrest. Both proteins have been shown to monitor tension across attached kinetochores and initiate mitotic arrest in response to loss of microtubule tension. As shown in Fig. 2, a slower migrating form of BubR1 was predominantly found in cells treated with higher doses of PBOX-6 ($\geq$ 5 μM) and PBOX-15 ($\geq$0.25 μM), which caused microtubule disruption as indicated by a significant increase in the percentage of cells arrested in the G_2M phase of the cell cycle (Fig. 1). It is well documented that this slower migrating form of BubR1 represents a hyperphosphorylated form of BubR1 (Chan et al., 1999; Li et al., 1999). Furthermore, hyperphosphorylated BubR1 has been related to an active mitotic checkpoint in nocodazole-blocked mitotic cells (Chan et al., 1999). Nocodazole-treated K562 cells were included as a positive control for BubR1 hyperphosphorylation (Fig. 2B). Unlike BubR1, the levels of Bub3 protein remained unchanged in G_2M-arrested K562 cells treated with PBOX-6 or -15 or nocodazole for 16 h (Fig. 2, A and B). Given that PBOX-15 is a more potent activator of the mitotic spindle checkpoint compared with PBOX-6, we next analyzed the effect of PBOX-15 (1 μM) on BubR1 phosphorylation over time. Again, cells treated with nocodazole (0.5 μM), a known stimulator of BubR1 phosphorylation, were used a positive control. The hyperphosphorylated form of BubR1 was most prominent 16 and 24 h after PBOX-15 and nocodazole treatment (Fig. 2C). At this time, the maximum G_2M cell cycle block was observed with 75% of PBOX-15-treated cells in the G_2M phase (Fig. 1B). It is noteworthy that the BubR1 protein was undetectable 48 h after PBOX-15 treatment in K562 cells (Fig. 2C). At this time, a significant decline in the percentage of G_2M-arrested cells was observed with a corresponding increase in the percentage of apoptotic cells (Fig. 1, B and C).

Inducibility of Mitotic Checking in Response to MTAs Correlated with Endogenous Levels of the Mitotic Spindle Checkpoint Proteins BubR1 and Bub3 in Human Cancer Cells. To further investigate the association of BubR1 and Bub3 with MTA-induced G_2M cell cycle arrest and apoptosis, we analyzed the absolute levels of both proteins and drug sensitivity to three MTAs (PBOX-6 and -15 and nocodazole) in five human cancer cell lines of different neoplastic origin. One cervical carcinoma (HeLa), two leukemia (K562 and HL-60), and two breast carcinoma (SK-BR-3 and MDA-MB-231) cell lines were tested. Effects of MTA treatment on BubR1 phosphorylation were also assessed in cells expressing detectable levels of BubR1. As shown in Fig. 3A, levels of the mitotic spindle checkpoint regulators BubR1 and Bub3 were dysregulated in human cancers. Levels of BubR1 and Bub3 were high in K562, HeLa, and MDA-MB-231 cells and low to undetectable in HL-60 and SK-BR-3 cells. We next examined the susceptibility of these cell lines to MTA (PBOX-6 and -15 and nocodazole)-induced G_2M cell cycle arrest and apoptosis to decipher any correlation with the mitotic spindle checkpoint. The extent of G_2M cell cycle arrest in response to depolymerization on the microtubules was highest in spindle checkpoint-proficient cells [K562 (Fig. 1), HeLa and MDA-MB-231 (Fig. 3B)] and lowest in spindle checkpoint-deficient cells (SK-BR-3 and HL-60) (Fig. 3B). Accordingly, the levels of MTA-induced apoptosis were inversely related to the levels of mitotic spindle checkpoint proteins in these cell lines. Specifically, in cells expressing high levels of BubR1 and Bub3, up to 75% of cells were arrested in the G_2M phase after a 24-h treatment with PBOX-6 or -15 or nocodazole. In direct contrast, in SK-BR-3 cells that express low levels of both BubR1 and Bub3, $\leq$35% cells were in the G_2M phase at 24 h, with levels decreasing dramatically to $<$3% 48 h after MTA treatment. Furthermore, after 24 h, there was no notable increase in the percentage of cells in the G_2M phase of HL-60 cells treated with MTAs compared with control-treated cells. A more detailed analysis of the effect of PBOX-6 and -15 on the cell cycle of HL-60 cells demonstrated a transient G_2M arrest commencing at 2 h and peaking at 8 h (Supplemental Fig. 3.1). A sustained G_2M arrest was not observed in these cells after MTA exposure, a finding consistent with the low levels of mitotic spindle checkpoint proteins found in HL-60 cells. In addition, after a 48-h exposure to MTAs, the maximum levels of apoptosis ($>$60%) were observed in spindle checkpoint-compromised SK-BR-3 and HL-60 cells (Fig. 3B). Apoptosis was determined by quantification of the pre-G_1 peak. In contrast, significantly lower levels of apoptosis ($\leq$ 37%) were

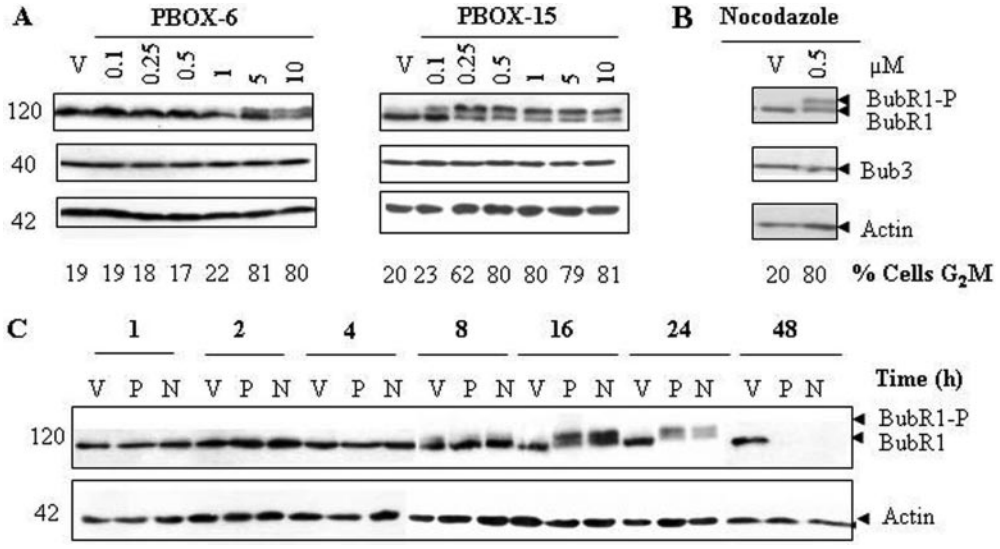

Fig. 2. BubR1 phosphorylation was associated with PBOX-induced G_2M cell cycle arrest in human chronic myeloid leukemia K562 cells. A, K562 cells in the log phase of growth were exposed to vehicle (V) [0.2% ethanol (v/v)] or PBOX-6 or -15 (0.1–10 μM) for 16 h. B, K562 cells were exposed to vehicle (V) (0.1% DMSO) or nocodazole (0.5 μM) for 16 h. C, K562 cells were exposed to vehicle (V) [0.2% ethanol (v/v)], PBOX-15 (P) (1 μM), or nocodazole (N) (0.5 μM) for 1 to 48 h. Whole-cell lysates were resolved by SDS-PAGE and probed with anti-BubR1 mouse mAb. Results are representative of three separate experiments. Blots were probed with anti-actin mAb as a loading control. BubR1-P, hyperphosphorylated form; BubR1, unphosphorylated form.

observed in the spindle checkpoint-proficient cells [K562 (Fig. 1), MDA-MB-231 and HeLa (Fig. 3B)]. This observed reduction in the percentage of apoptotic cells was accompanied by an increase in the percentage of cells remaining in the G_2M phase of the cell cycle. Apoptosis is characterized, at least in part, by the cleavage of PARP (116 kDa) into 89- and 24-kDa fragments that contain the active site and the DNA-binding domain of the enzyme, respectively. In this study, the onset of apoptosis correlated with PARP cleavage (Fig. 4A). Together, these findings suggest that a functional mitotic spindle checkpoint may contribute to a sustained G_2M cell cycle arrest after microtubule disruption induced by tubulin-targeting pyrrolo-1,5-benzoxazepines and the tubulin depolymerizer, nocodazole.

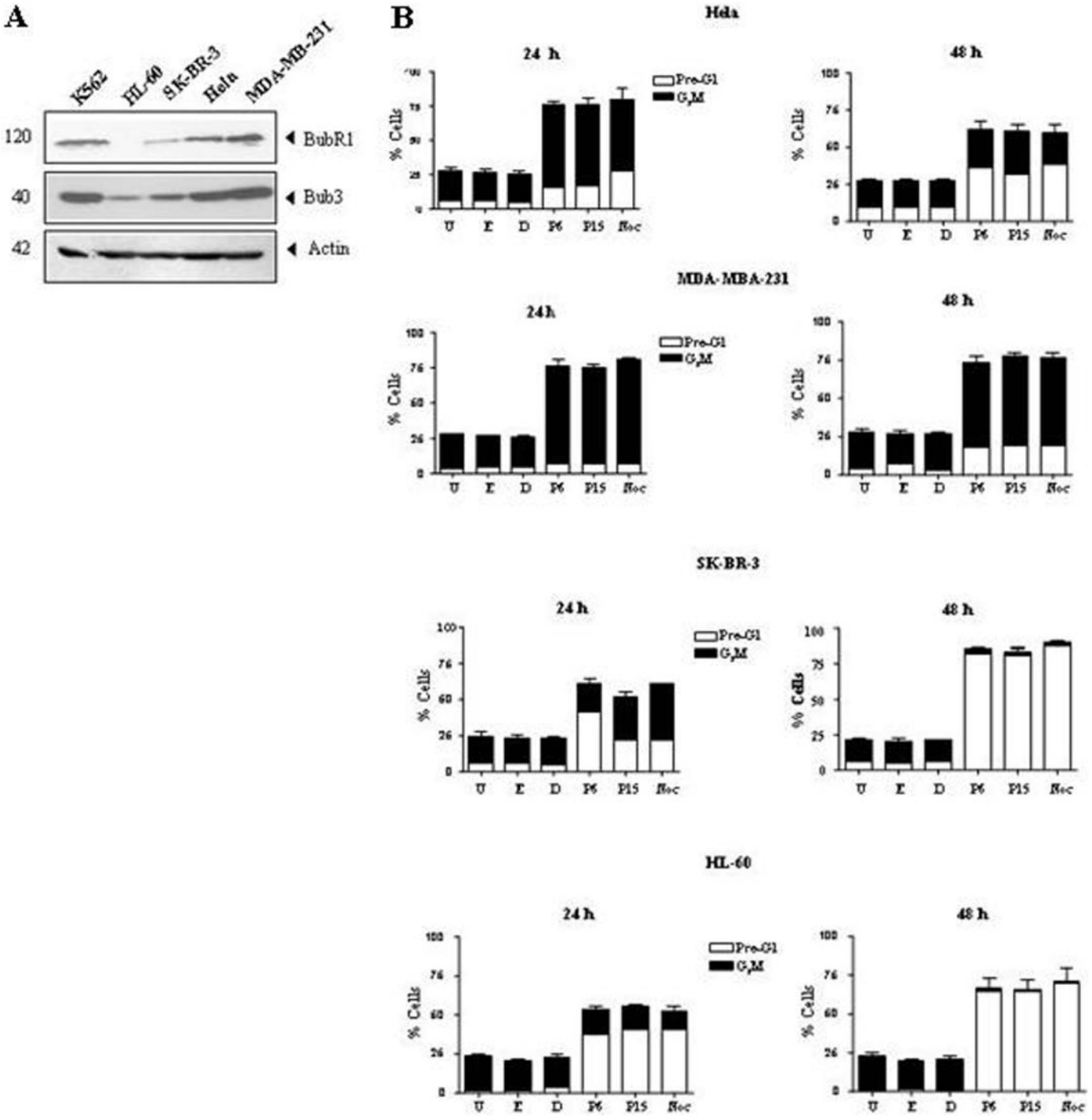

Fig. 3. Endogenous levels of mitotic spindle checkpoint proteins, BubR1 and Bub3, predict the type of cellular response to MTAs. A, equal amounts (50 μg) of whole-cell lysates were analyzed by Western blotting using anti-BubR1 and anti-Bub3 mAbs. Blots were probed with actin as a loading control. Results are representative of at least three separate experiments. B, subconfluent cells were treated with MTAs [P6, PBOX-6 (10 μM); P15, PBOX-15 (1 μM); or Noc, nocodazole (0.5 μM)] or relevant vehicle [E, 0.2% ethanol (v/v); D, 0.1% DMSO (v/v)] for the time indicated. Cells were then fixed, stained with PI, and analyzed by flow cytometry. Percentage apoptosis was determined by quantification of the pre-G_1 peak. The percentage of cells in the G_2M phase of the cell cycle is also indicated. Values represent the means for at least three separate experiments ± S.E.M.

We next examined the effects of PBOX and nocodazole exposure on BubR1 phosphorylation in cells expressing detectable levels of BubR1. Of the five cell lines tested in this study, MDA-MB-231 cells displayed the highest level of resistance to MTA (PBOX-6 and -15 and nocodazole) exposure with an average of 55% of cells remaining in the G_2M phase after 48 h. It is noteworthy that levels of the phosphorylated form of BubR1 remained high in these cells 48 h after MTA treatment, suggestive of an active spindle checkpoint (Fig. 4B). In HeLa cells, the decline in the percentage of G_2M-arrested cells from approximately 56% at 24 h to 25% 48 h after MTA exposure coincided with a significant decrease in BubR1 protein levels. In SK-BR-3 cells, BubR1 phosphorylation was again associated with MTA-induced G_2M arrest at 24 h. Furthermore, the decline in the percentage of G_2M-arrested SK-BR-3 cells 48 h after MTA treatment was once more associated with a reduction in BubR1 protein levels. It is worth noting that in contrast to K562 cells (Fig. 2) and MDA-MB-231 and HeLa cells (Fig. 4B), phosphorylation of BubR1 was not detected in SK-BR-3 cells treated with PBOX-6 for 24 h (Fig. 4B). However, at 24 h, PBOX-6 did not induce a G_2M cell cycle arrest in these cells (Fig. 3B). In contrast, treatment with PBOX-15 and nocodazole did induce both a G_2M cell cycle arrest and phosphorylation of BubR1 in SK-BR-3 cells. In addition, the ratio of the phosphorylated form of BubR1 to the unphosphorylated form of BubR1 was lowest in the SK-BR-3 cells compared with K562 (Fig. 2), MDA-MB-231, and HeLa cells at 24 h after MTA treatment (Fig. 4B). In accordance with this observation, the extent of G_2M cell cycle arrest was significantly less in SK-BR-3 (Fig. 3B) cells than that observed in K562 (Fig. 2), MDA-MB-231, and HeLa cells (Fig. 3B). Taken together, these findings confirm that BubR1 is required for the activation and maintenance of the mitotic spindle checkpoint in response to MTAs.

PBOX-15 Caused a Complete Depolymerization of the Microtubule Network and Altered Chromosome Alignment during Prometaphase and Metaphase. Next, we examined the effects of PBOX-15 on the morphology of the mitotic spindle and on the cellular localization pattern of BubR1 after loss of microtubule tension induced by PBOX-15 in HeLa cells. PBOX-15 can potently inhibit the assembly of tubulin in vitro as determined by changes in turbidity produced after the polymerization of tubulin (Mulligan et al.,

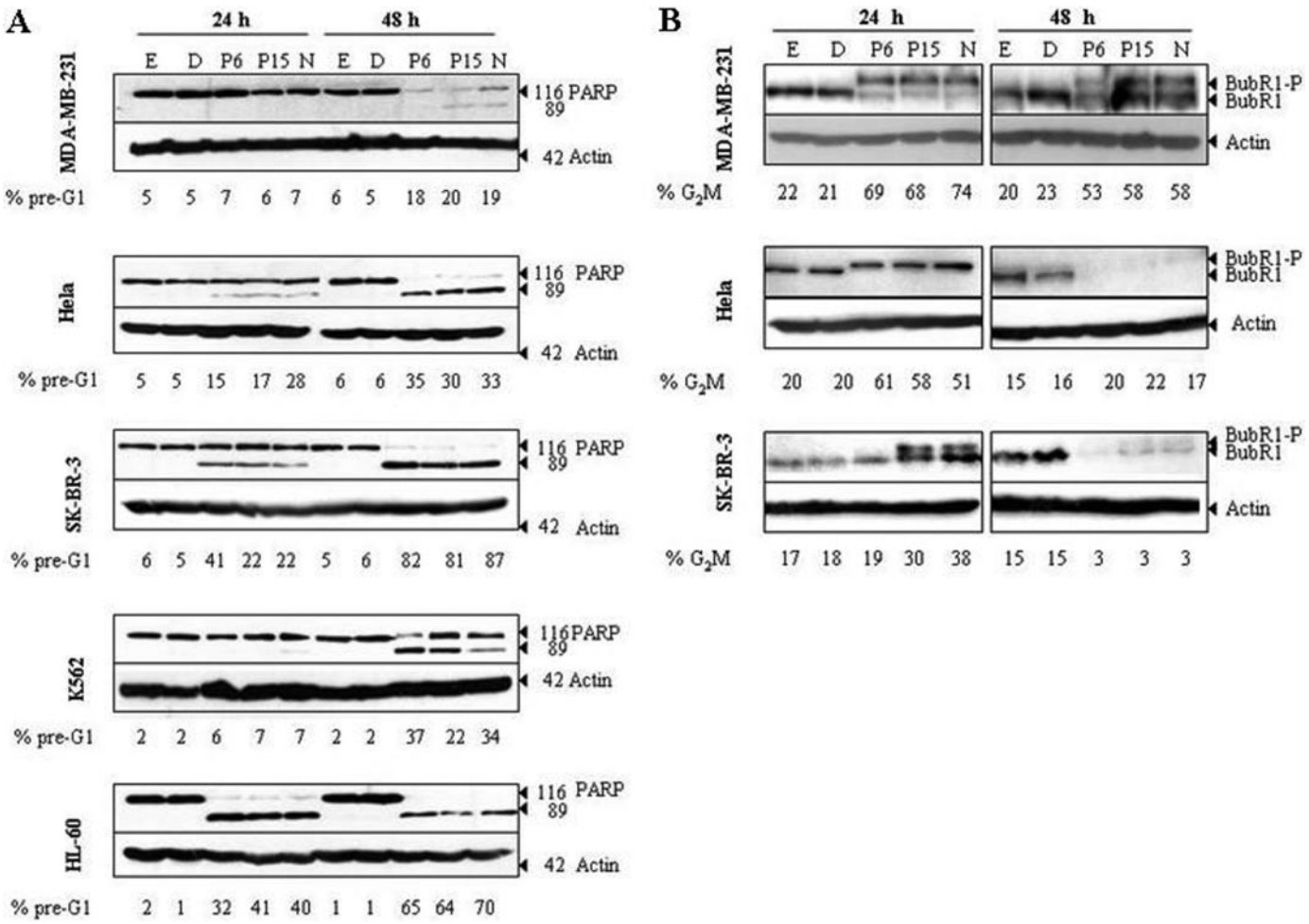

Fig. 4. Phosphorylation of BubR1 correlated with G_2M cell cycle arrest, and down-regulation of BubR1 correlated with apoptosis in human cancer cells treated with MTAs. Whole-cell extracts were prepared from each cell line after treatment with MTAs [P6, PBOX-6 (10 μM); P15, PBOX-15 (1 μM); N, nocodazole (0.5 μM)] or relevant vehicle [E, 0.2% ethanol (v/v); D, 0.1% DMSO (v/v)] for the time indicated. Lysates were resolved by SDS-PAGE and probed with anti-PARP (A) and anti-BubR1 mAbs (B). Blots were probed with anti-actin monoclonal antibody as a loading control. The mean percentages of cells in the pre-G_1 peak (apoptotic) and G_2M phase of the cell cycle are also indicated. Results shown are representative of three independent experiments.

2006). In addition, PBOX-15 disrupted the microtubule network of the breast carcinoma cell line, MCF-7, in interphase (Mulligan et al., 2006). Here, using confocal imagery, we demonstrate a complete depolymerization of the microtubule network in PBOX-15-arrested prometaphase and metaphase HeLa cells (Fig. 5). It is well accepted that in metaphase, BubR1 locates to the kinetochores during normal mitosis and mitotic arrest after mitotic insult by MTAs (Taylor et al., 2001). Therefore, it may be inferred that BubR1 staining in Fig. 5 depicts chromosomal location. In normal (control) prometaphase and metaphase, chromosomes are aligned and tightly organized around the metaphase plate. In PBOX-15-arrested prometaphase and metaphase cells, BubR1 staining was scattered and diffuse due to incorrect chromosome attachment/alignment because of loss of microtubule tension.

Gene Silencing of BubR1 by siRNA Led to Polyploidy after Mitotic Spindle Disruption in HeLa and MDA-MB-231 Cells. To further investigate the role of BubR1 in mitotic cell cycle arrest after mitotic spindle disruption by antimitotic PBOX compounds and nocodazole, endogenous levels of BubR1 were reduced using RNA interference. No significant difference in BubR1 knockdown levels were observed between HeLa cells exposed to the transfection complex containing BubR1 siRNA (30–100 nM) for 4 or 24 h (Fig. 6A). However, increased cell viability was observed in cells exposed to the transfection complex for 4 as opposed to 24 h (data not shown). Hence, for all subsequent experiments, cells were exposed to a transfection complex containing 50 nM siRNA duplexes for 4 h. The scrambled siRNA duplex (siRNA control) did not effect the expression levels of BubR1, verifying the specificity of the siRNA approach (Fig. 6A). A time-dependent reduction in BubR1 protein levels was observed in HeLa cells treated with BubR1 siRNA duplexes (Fig. 6B). A maximum reduction in BubR1 expression levels was observed 48 h after transfection, and levels remained low up to 72 h. We next used flow cytometry to determine whether suppression of BubR1 affected the cell cycle distribution of HeLa cells treated with PBOX-15 and nocodazole. As anticipated, down-regulation of BubR1 reduced the percentage of cells arrested in G_2M after MTA treatment (Fig. 6C). Similar results were obtained with PBOX-6 (data not shown). Depletion of BubR1 did not enhance the apoptotic efficacy of MTAs in HeLa cells (Fig. 6C). However, knockdown of BubR1 alone did induce up to 20% apoptosis at 3 days after transfection in HeLa cells. These results are in agreement with Kops et al. (2004), in which knockdown of BubR1 also caused cell death. Therefore, if the 20% cell death as a result of loss of BubR1 is accounted for, PBOX-15 and nocodazole were less effective at inducing apoptosis in BubR1-depleted cells. In addition, PARP cleavage was somewhat reduced in BubR1-depleted HeLa cells treated with MTAs compared with BubR1-expressing HeLa cells, confirming our hypothesis that artificial down-regulation of BubR1 impedes the apoptotic potential of MTAs (Fig. 7B). A subpopulation of HeLa cells exhibited a senescent-like growth arrest subsequent to PBOX-15 treatment because no increase in the apoptotic peak was observed up to 4 days after PBOX-15 treatment (Fig. 7A). Treatment with nocodazole

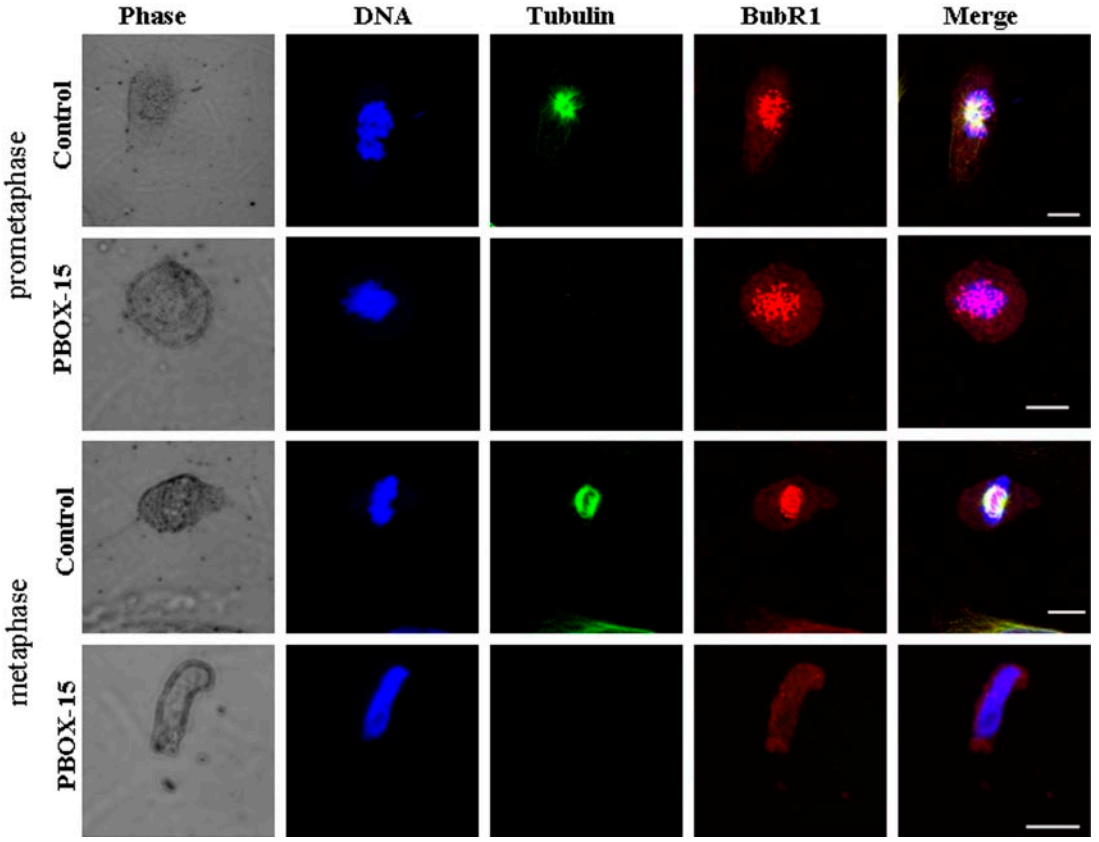

Fig. 5. Effects of PBOX-15 on the microtubule network and localization of BubR1 in prometaphase and metaphase cells. Phase contrast and confocal fluorescent images of normal (control) and PBOX-15 (1 μM)-treated HeLa cells. Projections of multiple confocal sections along z-axis show HeLa cells stained with DM1A (anti-tubulin, green), SBR1.1 (anti-BubR1, red), and Hoechst (blue). Scale bars, 10 μM.

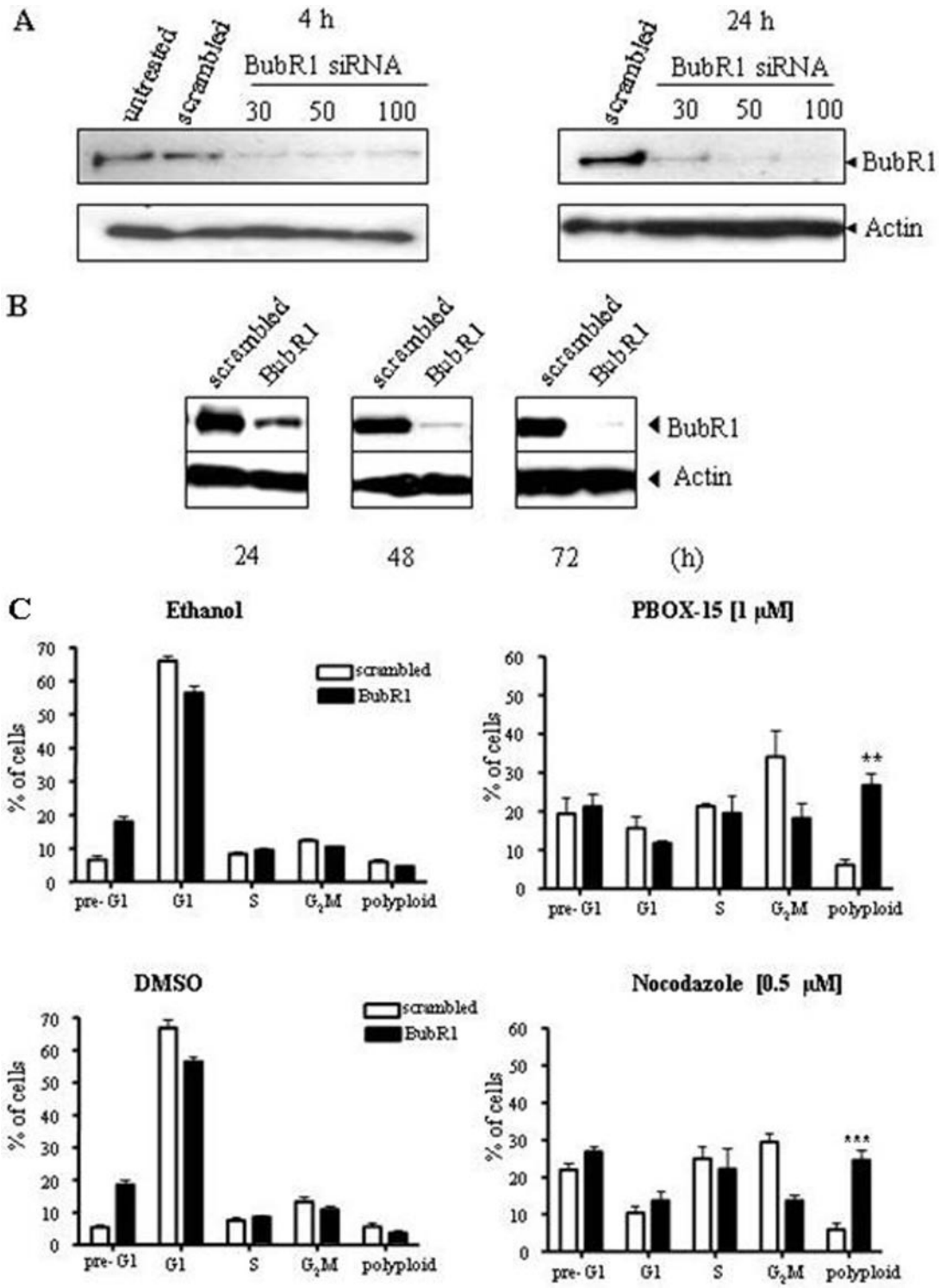

Fig. 6. siRNA repression of BubR1 led to increased polyploidy after mitotic spindle disruption in human cervical carcinoma-derived cells. A, HeLa cells were left untreated or exposed to siRNA duplexes for the time indicated, after which the medium was replaced with DMEM containing 20% FCS. Cells were harvested 48 h after transfection. B, cells were exposed to the indicated siRNA duplexes for 4 h. Cells were harvested at 24 to 72 h after transfection. Scrambled siRNA concentration is 100 nM (A) and 50 nM (B). A and B, equal amounts of whole-cell lysates were separated by SDS-PAGE and probed with anti-BubR1 mAb. Blots were probed with anti-actin mAb as a loading control. Results shown are representative of three separate experiments. C, HeLa cells were transfected with control (scrambled) or BubR1 siRNA duplexes at a final concentration of 50 nM for 4 h, cultured in DMEM with 20% FCS for a further 20 h, and subsequently treated with ethanol vehicle [0.2% (v/v)], DMSO [0.1% (v/v)], PBOX-15 (1 μM), or nocodazole (0.5 μM) and harvested after 48 h. Cell cycle analysis was performed on histograms of gated counts per DNA area (FL2-A). Relative percentage of cells with <2N (pre-G_1; apoptotic), 2N (G_0G_1), 4N (G_2M), or >4N (polyploid) DNA content were derived from the analysis of DNA histograms using the Cell Quest software. Results are representative of three separate experiments. Values represent the mean ± S.E.M. for at least three separate experiments. **, $P < 0.01$; and ***, $P < 0.001$; paired Student's t test.

produced similar results (data not shown). It is clearly evident from the representative histograms (Fig. 7A) that gene targeting of BubR1 did not enhance the apoptotic potential of MTAs, even after 4 days. In addition, knockdown of BubR1 resulted in a significant increase in the formation of polyploidy (a cell that contains greater than two full sets of chromosomes; DNA content > 4N) 48 h after microtubule disruption compared with control cells ($P < 0.01$; Student's t test; Fig. 6C). These polyploid cells continued to endoreplicate overtime forming cells with 16N DNA content after 4 days (Fig. 7A).

Next, given that the expression profile of Bub3 mirrored that of endogenous BubR1 in the cancer cell lines analyzed in this study (Fig. 3A), we sought to evaluate whether forced down-regulation of BubR1 would influence Bub3 protein levels. As depicted in Fig. 7B, Bub3 expression levels were not directly influenced by BubR1. Likewise, knockdown of BubR1 in *Xenopus laevis* egg extracts does not affect absolute Bub3 protein levels (Chen, 2002). These findings support the lack of involvement of BubR1 over Bub3 expression across species.

The effect of PBOX-15 on the microtubule network and morphology of BubR1-depleted cells was determined by confocal microscopy. As shown in Fig. 7C, PBOX-15 depolymer-

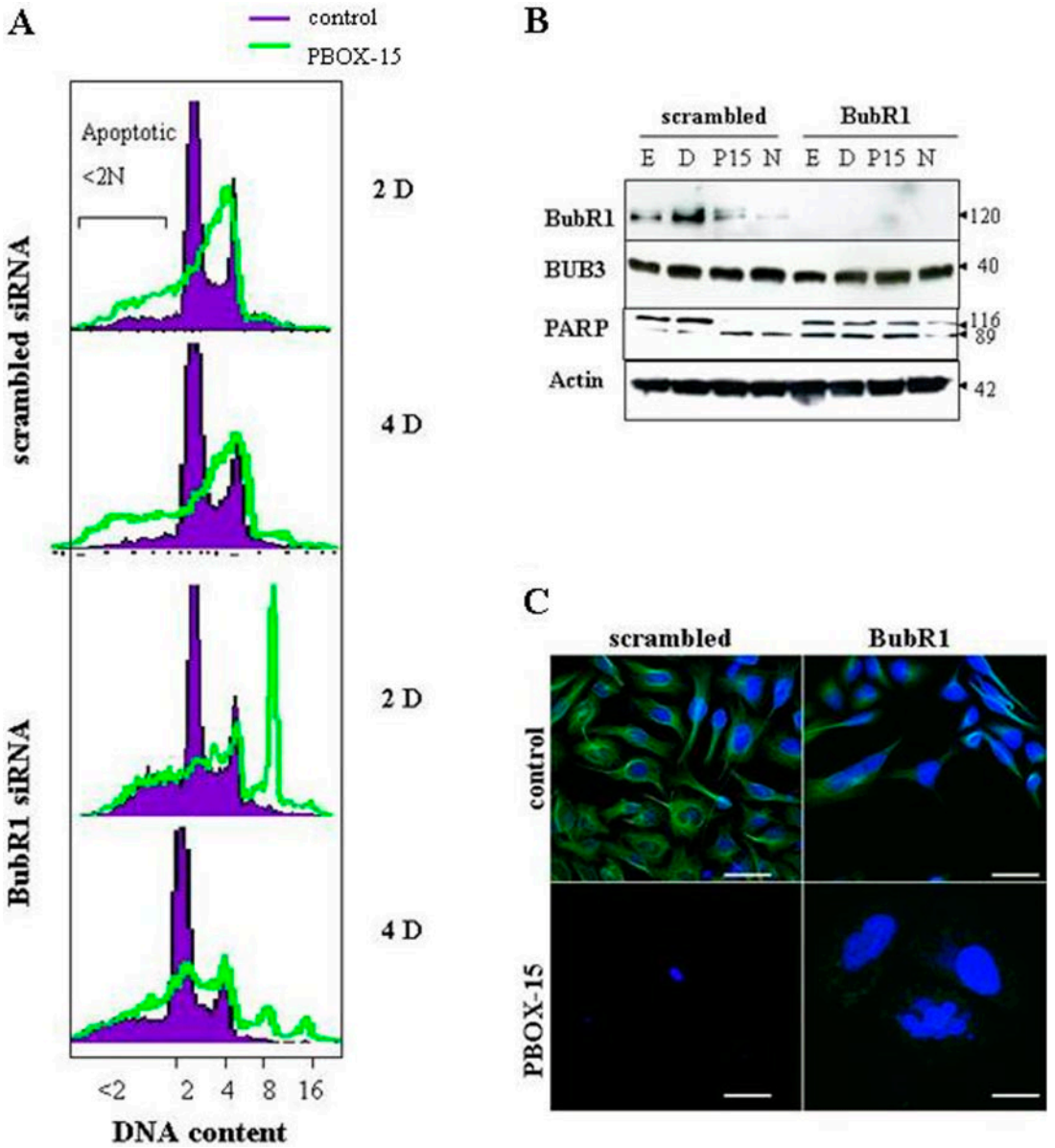

Fig. 7. Effects of BubR1 depletion of PBOX-15-induced cell death. HeLa cells were transfected with BubR1 or scrambled siRNA duplexes as described under *Materials and Methods*. After 24 h, cells were then treated with control vehicle [0.2% ethanol (v/v)] or PBOX-15 (1 μM) for the time indicated. A, representative overlays of log DNA histograms demonstrating the effect of PBOX-15 (open histograms) on HeLa cells transfected with BubR1 or scrambled siRNA complexes after 2 (2 D) and 4 (4 D) days. Vehicle-treated cells are represented with shaded histograms. DNA content of the cells is indicated [<2N (pre-G_1; apoptotic), 2N (G_0G_1), 4N (G_2M), or >4N (polyploidy)] below histograms and were derived using the Cell Quest software. B, Western blotting showing PARP cleavage and Bub3 protein levels in siRNA-transfected cells treated with ethanol vehicle (E), DMSO vehicle (D), PBOX-15 (P15), or nocodazole (N) for 2 days. Knockdown of BubR1 was confirmed by probing blots with anti-BubR1. Blots were probed with anti-actin as a loading control. C, siRNA-transfected cells were treated with either ethanol (control) or PBOX-15 for 4 days. Cells were then fixed and stained with Hoechst (blue) and anti-tubulin antibodies (green). Bar, 40 μM. All results shown are representative of at least three separate experiments.

ized the microtubule network of HeLa cells transfected with scrambled and BubR1 siRNA complexes. However, BubR1-depleted cells were giant-like in appearance and were either mono- or multinucleated because of aberrant cycling without cytokinesis.

To further confirm the importance of BubR1 protein levels in maintaining a stable mitotic arrest and preventing polyploidy, we down-regulated BubR1 protein levels by siRNA interference in a second cell line, MDA-MB-231. The specificity of the reaction was again confirmed by Western blot analysis of cells treated with BubR1 siRNA and a control scrambled sequence. As shown in Fig. 8, expression of BubR1 was substantially repressed in cells treated with BubR1 siRNA duplexes compared with control-treated cells. Again, as expected, down-regulation of BubR1 resulted in a significant increase in the formation of polyploid cells after mitotic release 48 h after PBOX-15 and nocodazole treatment ($P < 0.05$; Student's t test). These findings highlight the importance of BubR1 levels in the prevention of polyploidy after mitotic spindle disruption.

Discussion

Herein, we report that the mitotic spindle checkpoint regulators BubR1 and Bub3 were differentially expressed in human cancers. More importantly, the endogenous levels of the mitotic spindle checkpoint proteins directly correlated with the cellular response to microtubule disruption. The mitotic spindle checkpoint is a complex pathway conserved across species and monitors the metaphase to anaphase transition. The basic model for the spindle checkpoint defines that tension defects or unattached chromosomes activate the checkpoint delaying the onset of anaphase until such aberrations are corrected. The kinetochores attach chromosomes to the spindle. This aspect of spindle checkpoint is highly organized. The kinetochore assembly process has been carefully dissected using RNA interference coupled with quantitative optical sectioning microscopy. The checkpoint proteins Bub1, Cenp-F, BubR1, Cenp-E, Bub3, and MAD2 all transiently localize in sequence to the kinetochore (Chen, 2002; Johnson et al., 2004). After accurate chromosome alignment, the levels of the checkpoint proteins decline, and the cell cycle continues. Failure of the kinetochore to attach the sister chromatid in alignment on the mitotic spindle will trigger a "wait signal" and prevent anaphase onset. As mentioned, localization of the checkpoint proteins to the kinechore is an organized event and not a random process. Bub1 is required for localization of Cenp-F, BubR1, Cenp-E, and MAD2 (Johnson et al., 2004). However, repression of either Bub1 (Johnson et al., 2004) or Cenp-F (Holt et al., 2005) did not compromise spindle checkpoint function, suggesting multiple start points for the spindle checkpoint cascade. BubR1 is next in the checkpoint cascade promoting recruitment of Bub1, Bub3, Mad1, Mad2, and CENP-E (Chen, 2002). Hence, given that the two forefront proteins, Bub1 and Cenp-F, are indispensable for checkpoint function, considerable interest has escalated in the next candidate, BubR1.

Gene silencing of BubR1 impairs normal spindle checkpoint function (Kops et al., 2004). Documentation reporting affects of BubR1 depletion on spindle checkpoint function in response to mitotic insult is conflicting. In particular, suppression of BubR1 by siRNA interference inhibited paclitaxel-induced cell death in MCF-7 breast cancer cells (Sudo et al., 2004). In support of these findings, Shin et al. (2003) demonstrated that mutational and post-transcriptional inhibition of BubR1 reduced nocodazole-induced cytotoxicity by compromising mitotic arrest. However, in contrast to these results, the apoptotic efficacy of both paclitaxel and nocodazole was increased in HeLa cells after the siRNA-targeted down-regulation of BubR1 (Lee et al., 2004). These apparent discrepancies warranted the need for additional studies in both HeLa cells and other cell types to further elucidate the role played by BubR1 in MTA-induced cell death. In this study, we found that BubR1 is essential for a sustained mitotic checkpoint in response to loss of microtubule tension induced by a novel class of MTAs, the pyrrolo-1,5-benzoxazepines and the tubulin depolymerizer, nocodazole, in cells of different neoplastic origin.

First, results from unmanipulated cells suggested that absolute levels of BubR1 may determine the length of stay in G_2M. In support of our hypothesis, Meraldi et al. (2004) demonstrated that knockdown of BubR1 accelerates the normal progression of mitosis. Furthermore, in our studies, the MTA-induced G_2M block was maintained until endogenous levels of BubR1 protein became undetectable, and at this point, a marked increase in apoptosis was observed. BubR1 cellular levels inversely correlated with the onset of apoptosis. These results are in agreement with recent reports suggesting that degradation of BubR1 by both a caspase-dependent (Kim et al., 2005) and a ubiquitin-dependent (Shin et al., 2003) proteosome pathway were associated with release from mitotic block after prolonged spindle damage. Collectively, these results suggest that endogenous levels of BubR1 may predict the apoptotic efficacy and potential chemotherapeutic benefit of MTAs in human cancers. In support of this hypothesis, BubR1 was found to be overexpressed in a cohort of 43 gastric carcinomas (Grabsch et al., 2003). It is noteworthy that paclitaxel failed in clinical trials in patients with gastric carcinoma (Garcia et al., 2001). An overactive mitotic checkpoint may contribute to paclitaxel resistance in gastric carcinomas, among others.

We also report that expression levels of Bub3 mirrored those of BubR1 in the cells lines tested. This finding is interesting because both proteins are believed to evoke a spindle checkpoint in response to loss of spindle tension (Logarinho et al., 2004). Therefore, it was not unexpected that the weakest mitotic response to MTA-induced loss of microtubule tension was observed in the cell lines expressing the lowest levels of Bub3 and BubR1. However, mitotic insult or the onset of apoptosis did not alter the expression levels or post-translational modification in terms of phosphorylation, of Bub3. As reported herein and elsewhere (Meraldi et al., 2004), forced down-regulation of BubR1 did not influence total cellular Bub3 levels, suggesting that Bub3 protein levels are not directly controlled by BubR1.

We next sought to determine whether forced down-regulation of BubR1 through the RNA interference strategy could induce a similar phenotype in terms of apoptotic susceptibility to MTAs as cells that had evolved to express low levels of BubR1. Gene silencing of BubR1 significantly reduced the accumulation of cells in the G_2M phase in cells derived from both a cervical and a breast carcinoma in response to mitotic insult. These results support previous studies demonstrating that BubR1 is essential for maintaining a mitotic arrest in

response to microtubule disruption induced by the tubulin polymerizer, paclitaxel (Sudo et al., 2004). In our studies, knockdown of BubR1 did not enhance the apoptotic efficacy of the tubulin-targeting PBOX compounds or nocodazole in human cancer cells. Depolymerization of the microtubules and depletion of BubR1 led to incomplete cytokinesis. Our results compliment those of Kops et al. (2004), in which giant multinucleated cells were observed in BubR1-depleted HeLa cells after continued exposure to a structurally different tubulin depolymerizer, Colcemid. Taken together, these obser-

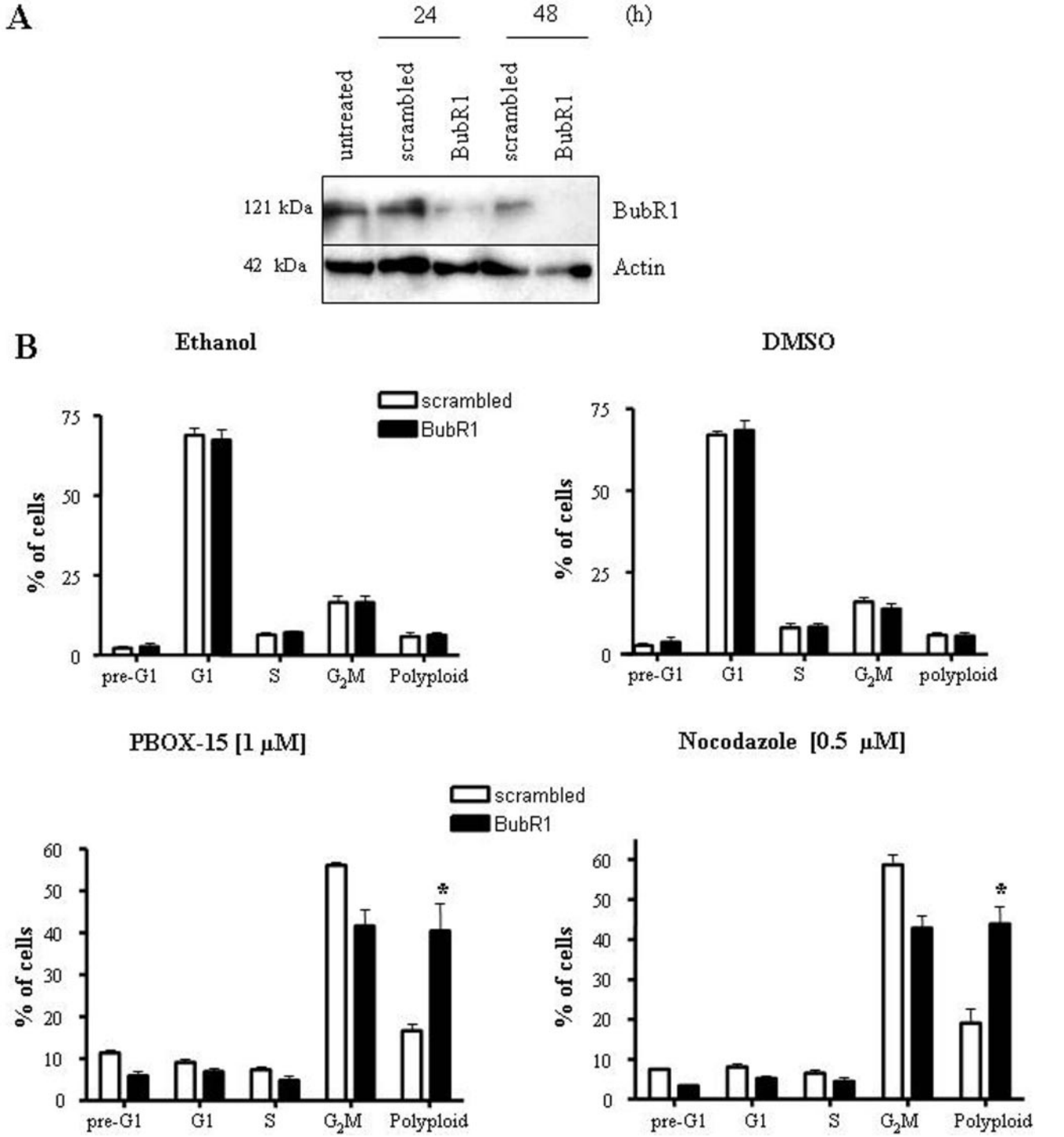

Fig. 8. Targeted inhibition of BubR1 increased polyploidy in human MDA-MB-231 breast carcinoma-derived cells after a prolonged mitotic disruption. Cells were transfected with 50 nM BubR1 or scrambled siRNA duplexes for 4 h and cultured in DMEM supplemented with 20% FCS thereafter. A, Western blot showing repression of BubR1 at 24 and 48 h after transfection. Actin was used as a loading control. B, 24 h after transfection, cells were treated with relevant vehicle, PBOX-15 (1 μM) or nocodazole (0.5 μM) for 48 h. Cells were then fixed, stained with PI, and analyzed by flow cytometry. Cell cycle analysis was performed on histograms of gated counts per DNA area (FL2-A). Relative percentages of cells with $<$2N (pre-G_1; apoptotic), 2N (G_0G_1), 4N (G_2M), and $<$4N (polyploid) DNA content were derived from the analysis of DNA histograms using the Cell Quest software. Results are representative of three separate experiments. Values represent the mean $\pm$ S.E.M. for at least three separate experiments ($*$, $P < 0.05$; paired Student's t test).

vations imply that BubR1 not only functions as a guardian of the mitotic spindle but also as a key regulator in the execution of cytokinesis.

Further studies investigating the role of BubR1 in cytokinesis are warranted before advances can be made in terms of augmenting MTA-induced cytotoxicity. Specifically, it would be interesting to determine whether phosphorylation of BubR1 is necessary for its role in cytokinesis. Once clarified, this knowledge can be exploited to enhance the apoptotic efficacy of MTAs and other drugs impeded by a prolonged mitotic checkpoint. The Aurora B kinase inhibitor, ZM447439, is a potent inhibitor of BubR1 phosphorylation and spindle checkpoint activation (Ditchfield et al., 2003). It may therefore be of interest to determine any therapeutic benefits in combining ZM447439 with MTAs, including the pyrrolo-1,5-benzoxazepines.

In conclusion, the pyrrolo-1,5-benzoxazepines represent a novel class of MTAs for the effective treatment of carcinomas expressing low endogenous levels of the mitotic spindle checkpoint regulator, BubR1. Moreover, reduction of BubR1 may form a critical link between the spindle checkpoint and induction of apoptosis by tubulin targeting pyrrolo-1,5-benzoxazepines and other MTAs.

Acknowledgments

We thank Orla Hanrahan (School of Biochemistry and Immunology, Trinity College, Dublin, UK) for technical assistance on the confocal microscope and Stephen Taylor (School of Biological Sciences, University of Manchester, Manchester, UK) for helpful advice on achieving optimal tubulin and chromosome staining.

References

Acquaviva C, Herzog F, Kraft C, and Pines J (2004) The anaphase promoting complex/cyclosome is recruited to centromeres by the spindle assembly checkpoint. *Nat Cell Biol* **6:**892–898.

Campiani G, Fiorini I, De Filippis MP, Ciani SM, Garofalo A, Nacci V, Giorgi G, Sega A, Botta M, Chiarini A, et al. (1996) Cardiovascular characterization of pyrrolo[2,1-*d*][1,5]benzothiazepine derivatives binding selectively to the peripheral-type benzodiazepine receptor (PBR): from dual PBR affinity and calcium antagonist activity to novel and selective calcium entry blockers. *J Med Chem* **39:**2922–2938.

Chan GK, Jablonski SA, Sudakin V, Hittle JC, and Yen TJ (1999) Human BUBR1 is a mitotic checkpoint kinase that monitors CENP-E functions at kinetochores and binds the cyclosome/APC. *J Cell Biol* **146:**941–954.

Chen RH (2002) BubR1 is essential for kinetochore localization of other spindle checkpoint proteins and its phosphorylation requires Mad1. *J Cell Biol* **158:**487–496.

Cleveland DW, Mao Y, and Sullivan KF (2003) Centromeres and kinetochores: from epigenetics to mitotic checkpoint signaling. *Cell* **112:**407–421.

Ditchfield C, Johnson VL, Tighe A, Ellston R, Haworth C, Johnson T, Mortlock A, Keen N, and Taylor SS (2003) Aurora B couples chromosome alignment with anaphase by targeting BubR1, Mad2, and Cenp-E to kinetochores. *J Cell Biol* **161:**267–280.

Doncic A, Ben-Jacob E, and Barkai N (2005) Evaluating putative mechanisms of the mitotic spindle checkpoint. *Proc Natl Acad Sci U S A* **102:**6332–6337.

Garcia AA, Leichman CG, Lenz HJ, Baranda J, Lujan R, Casagrande Y, and Leichman L (2001) Phase II trial of outpatient schedule of paclitaxel in patients with previously untreated metastatic, measurable adenocarcinoma of the stomach. *Jpn J Clin Oncol* **31:**275–278.

Grabsch H, Takeno S, Parsons WJ, Pomjanski N, Boecking A, Gabbert HE, and Mueller W (2003) Overexpression of the mitotic checkpoint genes BUB1, BUBR1, and BUB3 in gastric cancer-association with tumour cell proliferation. *J Pathol* **200:**16–22.

Greene LM, Fleeton M, Mulligan J, Gowda C, Sheahan BJ, Atkins GJ, Campiani G, Nacci V, Lawler M, Williams DC, et al. (2005) The pyrrolo-1,5-benzoxazepine, PBOX-6, inhibits the growth of breast cancer cells in vitro independent of estrogen receptor status and inhibits breast tumour growth *in vivo*. *Oncol Rep* **14:**1357–1363.

Holt SV, Vergnolle MA, Hussein D, Wozniak MJ, Allan VJ, and Taylor SS (2005) Silencing Cenp-F weakens centromeric cohesion, prevents chromosome alignment and activates the spindle checkpoint. *J Cell Sci* **118:**4889–4900.

Jordan MA (2002) Mechanism of action of antitumor drugs that interact with microtubules and tubulin. *Curr Med Chem Anticancer Agents* **2:**1–17.

Johnson VL, Scott MI, Holt SV, Hussein D, and Taylor SS (2004) Bub1 is required for kinetochore localization of BubR1, Cenp-E, Cenp-F and Mad2, and chromosome congression. *J Cell Sci* **117:**1577–1589.

Kim M, Murphy K, Liu F, Parker SE, Dowling ML, Baff W, and Kao GD (2005) Caspase-mediated specific cleavage of BubR1 is a determinant of mitotic progression. *Mol Cell Biol* **25:**9232–9248.

Kops GJ, Foltz DR, and Cleveland DW (2004) Lethality to human cancer cells through massive chromosome loss by inhibition of the mitotic checkpoint. *Proc Natl Acad Sci U S A* **101:**8699–8704.

Lee EA, Keutmann MK, Dowling ML, Harris E, Chan G, and Kao GD (2004) Inactivation of the mitotic checkpoint as a determinant of the efficacy of microtubule-targeted drugs in killing human cancer cells. *Mol Cancer Ther* **3:**661–669.

Li W, Lan Z, Wu H, Wu S, Meadows J, Chen J, Zhu V, and Dai W (1999) BUBR1 phosphorylation is regulated during mitotic checkpoint activation. *Cell Growth Differ* **10:**769–775.

Logarinho E, Bousbaa H, Dias JM, Lopes C, Amorim I, Antunes-Martins A, and Sunkel CE (2004) Different spindle checkpoint proteins monitor microtubule attachment and tension at kinetochores in *Drosophila* cells. *J Cell Sci* **117:**1757–1771.

Meraldi P, Draviam VM, and Sorger PK (2004) Timing and checkpoints in the regulation of mitotic progression. *Dev Cell* **7:**45–60.

Mc Gee MM, Campiani G, Ramunno A, Fattorusso C, Nacci V, Lawler M, Williams DC, and Zisterer DM (2001) Pyrrolo-1,5-benzoxazepines induce apoptosis in chronic myelogenous leukemia (CML) cells by bypassing the apoptotic suppressor bcr-abl. *J Pharmacol Exp Ther* **296:**31–40.

Mc Gee MM, Campiani G, Ramunno A, Nacci V, Lawler M, Williams DC, and Zisterer DM (2002b) Activation of the c-Jun N-terminal kinase (JNK) signaling pathway is essential during PBOX-6-induced apoptosis in chronic myelogenous leukemia (CML) cells. *J Biol Chem* **277:**18383–18389.

Mc Gee MM, Greene LM, Ledwidge S, Campiani G, Nacci V, Lawler M, Williams DC, and Zisterer DM (2004) Selective induction of apoptosis by the pyrrolo-1,5-benzoxazepine 7-[[dimethylcarbamoyl]oxy]-6-(2-naphthyl) pyrrol-[2,1-d] (1,5)-benzoxazepine (PBOX-6) in Leukemia cells occurs via the c-Jun NH2-terminal kinase-dependent phosphorylation and inactivation of Bcl-2 and Bcl-XL. *J Pharmacol Exp Ther* **310:**1084–1095.

Mc Gee MM, Hyland E, Campiani G, Ramunno A, Nacci V, and Zisterer DM (2002a) Caspase-3 is not essential for DNA fragmentation in MCF-7 cells during apoptosis induced by the pyrrolo-1,5-benzoxazepine, PBOX-6. *FEBS Lett* **515:**66–70.

Mollinedo F and Gajate C (2003) Microtubules, microtubule-interfering agents and apoptosis. *Apoptosis* **8:**413–450.

Mulligan JM, Greene LM, Cloonan S, Mc Gee MM, Onnis V, Campiani G, Fattorusso C, Lawler MP, Williams C, and Zisterer DM (2006) Identification of tubulin as the molecular target of pro-apoptotic pyrrolo-1,5-benzoxazepines. *Mol Pharmacol* **70:**60–70.

Ofir R, Seidman R, Rabinski T, Krup M, Yavelsky V, Weinstein Y, and Wolfson M (2002) Taxol-induced apoptosis in human SKOV3 ovarian and MCF7 breast carcinoma cells is caspase-3 and caspase-9 independent. *Cell Death Differ* **9:**636–642.

Peters JM (2002) The anaphase-promoting complex: proteolysis in mitosis and beyond. *Mol Cell* **9:**931–943.

Shin HJ, Baek KH, Jeon AH, Park MT, Lee SJ, Kang CM, Lee HS, Yoo SH, Chung DH, Sung YC, et al. (2003) Dual roles of human BubR1, a mitotic checkpoint kinase, in the monitoring of chromosomal instability. *Cancer Cell* **4:**483–497.

Sudo T, Nitta M, Saya H, and Ueno NT (2004) Dependence of paclitaxel sensitivity on a functional spindle assembly checkpoint. *Cancer Res* **64:**2502–2508.

Tang C, Willingham MC, Reed JC, Miyashita T, Ray S, Ponnathpur V, Huang Y, Mahoney ME, Bullock G, and Bhalla K (1994) High levels of p26BCL-2 oncoprotein retard Taxol-induced apoptosis in human pre-B leukemia cells. *Leukemia* **8:**1960–1969.

Taylor SS, Hussein D, Wang Y, Elderkin S, and Morrow CJ (2001) Kinetochore localisation and phosphorylation of the mitotic checkpoint components Bub1 and BubR1 are differentially regulated by spindle events in human cells. *J Cell Sci* **114:**4385–4395.

Yu D, Jing T, Liu B, Yao J, Tan M, McDonnell TJ, and Hung MC (1998) Overexpression of ErbB2 blocks Taxol-induced apoptosis by upregulation of p21Cip1, which inhibits p34Cdc2 kinase. *Mol Cell* **2:**581–591.

Zisterer DM, Campiani G, Nacci V, and Williams DC (2000) Pyrrolo-1,5-benzoxazepines induce apoptosis in HL-60, Jurkat, and Hut-78 cells: a new class of apoptotic agents. *J Pharmacol Exp Ther* **293:**48–59.

Address correspondence to: Dr. Lisa Greene, School of Biochemistry and Immunology, Trinity College, Dublin 2, United Kingdom. E-mail: greeneli@tcd.ie